

# Torsional potentials of glyoxal, oxalyl halides and their thiocarbonyl derivatives: Challenges for popular density functional approximations.

Diana N. Tahchieva, Dirk Bakowies, Raghunathan Ramakrishnan, and O. Anatole von Lilienfeld\*

*Institute of Physical Chemistry and National Center for Computational Design and Discovery of Novel Materials (MARVEL), Department of Chemistry, University of Basel, Klingelbergstrasse 80, CH-4056 Basel, Switzerland*

E-mail: anatole.vonlilienfeld@unibas.ch

## Abstract

The reliability of popular density functionals was studied for the description of torsional profiles of 36 molecules: glyoxal, oxalyl halides and their thiocarbonyl derivatives. HF and eighteen functionals of varying complexity, from local density to range-separated hybrid approximations and double-hybrid, have been considered and benchmarked against CCSD(T)-level rotational profiles. For molecules containing heavy halogens, all functionals except M05-2X and M06-2X fail to reproduce barrier heights accurately and a number of functionals introduce spurious minima. Dispersion corrections show no improvement. Calibrated torsion-corrected atom-centered potentials rectify the shortcomings of PBE and also improve on  $\sigma$ -hole based intermolecular binding in dimers and crystals.

## 1 Introduction

Rotational barriers play a crucial role in the dynamical mechanism of chemical reactions and processes, and influence a plethora of molecular properties and phenomena including fluorescence emission intensity,<sup>1</sup> intersystem crossing<sup>2</sup> and protein folding.<sup>3</sup> A quantitative description of torsional profiles in conjugated systems is often difficult to achieve in an experi-

ment, but high-level *ab-initio* methods can provide significant insight.<sup>4-9</sup> It is particularly important that these numerical approaches yield accurate inter-atomic potentials, as chemical reactions often exhibit complex transition pathways with multiple local minima; notable examples being Diels-Alder reactions, which are often highly regio- and stereoselective.<sup>10</sup> Coupled-cluster theory has emerged as a highly accurate method and is often used as a reference for benchmarking more approximate approaches. However, its computational complexity limits its use to relatively small molecules. Density functional theory (DFT), on the other hand, often offers good computational efficiency and reliability. Various DFT functionals have in fact shown promising performance for torsional profiles, but the inclusion of exact exchange appears to be important for  $\pi$ -conjugated systems.<sup>5,11</sup>

An overview of the existing literature indicates a severe lack of chemical diversity in systems studied so far (Fig. 1). Most research thus far has been limited to first and second row elements in the periodic table<sup>4,8,9,11-126</sup> and only a few studies considered molecules with other atom types, such as Br,<sup>76,101</sup> Ge,<sup>70</sup> As,<sup>70</sup> Se<sup>115</sup> and Te<sup>127</sup> (see Figure 1).

In this work, we assess the accuracy of a large range of popular density functionals for the de-

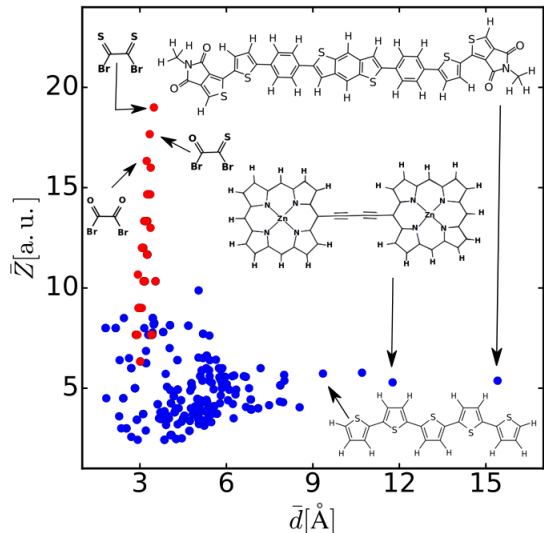


Figure 1: Chemical diversity of torsional potentials in molecules studied in the literature<sup>4,8,9,11–127</sup> (blue) and in this work (red). Vertical and horizontal axes correspond to averaged atomic charges and inter-atomic distances, respectively. Select examples are shown as insets.

scription of single bond torsions in glyoxal, oxalyl and thiocarbonyl halides. Our focus is on extending compositional diversity, including heavier halogens (up to Br) in a conjugated carbonyl and thiocarbonyl scaffold (Fig. 1 in red). The effect of dispersion corrections on torsional profiles is studied as well as custom-tailored atom centered potentials. The latter are shown to also improve the description of  $\sigma$ -hole based intermolecular binding.

## 2 Computational details

Torsional energy profiles  $E(\Theta)$  were obtained through restricted geometry optimizations in which the torsional angle  $\Theta = \Theta_{XCCY} = \Theta_{ACCB}$  ( $A, B$ : oxygen or sulfur,  $X, Y$ : hydrogen or halogen) is kept constant and carbon atoms remain in the plane of their three bonded neighbors. The entire range of  $0^\circ < \Theta < 180^\circ$  was scanned in steps of  $\Delta\Theta = 20^\circ$ . Note that  $E(360^\circ - \Theta) = E(\Theta)$ , follows from the applied constraints. Calculations were car-

ried out with Gaussian09,<sup>128</sup> using Hartree-Fock as well as the following density functional approximations: LDA (SVWN5<sup>129,130</sup>), GGA (PW91,<sup>131</sup> PBE,<sup>132</sup> BLYP,<sup>133,134</sup> BP86<sup>133,135</sup>), mGGA (TPSS,<sup>136</sup> M06L<sup>137</sup>), hGGA (PBE0,<sup>138</sup> B3LYP<sup>133,134,139</sup>), mhGGA (M05,<sup>140</sup> M06,<sup>141</sup> M05-2X,<sup>142</sup> M06-2X,<sup>141</sup> M06-HF<sup>141</sup>), RS (CAM-B3LYP,<sup>143</sup> M11<sup>144</sup>), double hybrid (B2PLYP,<sup>145</sup> DSD-PBEP86(B3BJ)<sup>146</sup>). Note that the DSD-PBEP86 functional has been parameterized for use with D3BJ correction and the expected accuracy of the double hybrid for non-bonding interactions cannot be obtained without the dispersion add-on.<sup>146</sup> The def2QZVPP<sup>147</sup> basis set was used throughout and parametric dispersion corrections (D3<sup>148</sup>) were used in some cases.

Additional plane-wave (PW) calculations were carried out for the PBE and BLYP functionals, using VASP<sup>149,150</sup> and CPMD,<sup>151</sup> respectively. MBD (Many Body Dispersion,<sup>152</sup> for PBE) and DCACP<sup>153,154</sup> (Dispersion Corrected Atom-Centered Potential, for BLYP) corrections were used as indicated in Section 3. MBD calculations were carried out using VASP in a box with size  $14 \times 14 \times 10 \text{ \AA}^3$  ( $1 \times 1 \times 1$   $\Gamma$ -centered k-point grid) and a cutoff of 600 eV. DCACP energies were calculated using a unit cell of  $(14 \text{ \AA})^3$  and a cutoff of 200 Ry with isolated boundary conditions.

Torsion corrected atom-centered potentials (TCACP) were constructed for PBE in analogy to other ACPs, following previously introduced optimization procedures.<sup>155,156</sup> The TCACP is added to Goedecker’s norm-conserving potentials<sup>157</sup> and shares the analytical form of its non-local part (Eq. 1).

$$V_I^{\text{TCACP}}(r, r') = \sum_{m=-l}^{+l} Y_{lm}(\hat{\mathbf{r}}) p_l(r) h_{11}^l p_l(r') Y_{lm}^*(\hat{\mathbf{r}}'), \quad (1)$$

with normalized projector  $p_l(r) \propto r^l \exp[-\frac{r^2}{2r_l^2}]$ .  $l$  denotes angular momentum (here  $l = 3$ ),  $\hat{\mathbf{r}}$  is the unit vector in the direction of  $\mathbf{r}$ ,  $r = |\mathbf{r} - \mathbf{R}_I|$  is the distance from the position of the nucleus  $I$  and  $Y_{lm}$  is a spherical harmonic. The parameters  $h_{11}^{l=3}$  and  $r_l$  are generated by minimizing

a penalty function  $P$ , which has the following form:

$$P = \frac{1}{N} \sum_i^N |E_i^{\text{CCSD(T)}} - E_i^{\text{PBE+TCACP}}|, \quad (2)$$

where  $i$  runs over all  $N = 90$  conformations used in the training set. The penalty is minimized using the Nelder-Mead simplex-downhill algorithm,<sup>153,156,158</sup> optimizing parameters corresponding to distance<sup>157</sup>  $r_{l=3}$  from the position of the nuclei and amplitude<sup>157</sup>  $h_{11}^{l=3}$ . Parameterization of TCACPs was carried out with CPMD using a box size of  $(14 \text{ \AA})^3$  and a 150 Ry cutoff with isolated boundary conditions.

Binding energies with TCACPs were calculated using a cutoff of 150 Ry and cell dimensions of  $24 \times 17 \times 14 \text{ \AA}^3$  for oxalyl bromide-water and of  $26 \times 19 \times 14 \text{ \AA}^3$  for the oxalyl bromide dimer. Cohesive energies as a function of a lattice scan were calculated for the oxalyl bromide crystal structure (2 molecules/unit cell) using Quantum Espresso<sup>159</sup> (PBE, PBE+TCACP) and VASP (PBE+MBD) with a  $3 \times 3 \times 3$   $\Gamma$ -centered k-point grid and a cutoff of 200 Ry and 600 eV, respectively. Experimental data was used for the crystal structure geometry and the initial unit cell dimensions, which was subsequently multiplied by a scaling factor  $f$ , ranging from 0.85 to 1.5.

CCSD(T)<sup>160,161</sup> energies were calculated using Molpro<sup>162</sup> and correlation-consistent basis sets<sup>163,164</sup> for M05-2X optimized geometries. CCSD(T)-F12<sup>165</sup> energies using cc-pVTZ-F12<sup>166</sup> basis sets (including effective core potentials (ECP) for Br<sup>167</sup>) were calculated with Molpro<sup>168</sup> for the same M05-2X geometries.

## 3 Results and Discussion

### 3.1 CCSD(T) convergence test

CCSD(T), often considered to be the gold standard of quantum chemistry, has been chosen as a reference level to judge the quality of density functional calculations. A basis set convergence analysis has been performed for a few represen-

Table 1: CCSD(T) basis set convergence: Potential energy difference of oxalyl bromide between dihedral angles  $\Theta = 80^\circ$  and  $\Theta = 180^\circ$  (in kcal/mol). Yellow colouring shows the reference method used in this study.

Scheme A Valence <i>sp</i> electrons correlated			Scheme B Valence <i>sp</i> and 3 <i>d</i> (Br) electrons correlated		
X	cc-pVXZ	aug-cc-pVXZ	X	cc-pVXZ	aug-cc-pVXZ
OSC <sub>2</sub> HBr (class I)					
D	4.30	3.46	D	4.34	3.46
T	3.62	3.58	T	3.68	3.72
Q	3.56	3.55	Q	3.56	3.86
5	3.53	3.46	5	3.60	3.74
CBS (Q5)	3.57	3.63	CBS (Q5)	3.60	3.63
CCSD(T)-F12	3.52	-	CCSD(T)-F12	3.51	-
(VTZ-F12); Ansatz 3C(FIX)			(VTZ-F12); Ansatz 3C(FIX)		
O <sub>2</sub> C <sub>2</sub> Br <sub>2</sub> (class II)					
D	1.86	0.41	D	1.73	0.41
T	0.61	0.53	T	0.61	0.62
Q	0.49	0.54	Q	0.52	0.81
5	0.47	0.55	5	0.47	0.71
CBS (Q5)	0.51	0.56	CBS (Q5)	0.47	0.58
CCSD(T)-F12	0.47	-	CCSD(T)-F12	0.46	-
(VTZ-F12); Ansatz 3C(FIX)			(VTZ-F12); Ansatz 3C(FIX)		
S <sub>2</sub> C <sub>2</sub> Br <sub>2</sub> (class III)					
D	-3.05	-3.23	D	-2.98	-3.19
T	-3.13	-2.62	T	-3.11	-2.55
Q	-2.57	-2.32	Q	-2.48	-2.09
5	-2.40	-2.26	5	-2.36	-2.11
CBS (Q5)	-2.19	-2.18	CBS (Q5)	-2.21	-2.11
CCSD(T)-F12	-2.34	-	CCSD(T)-F12	-2.35	-
(VTZ-F12); Ansatz 3C(FIX)			(VTZ-F12); Ansatz 3C(FIX)		

tative cases with different shapes of torsional potentials (O<sub>2</sub>C<sub>2</sub>Br<sub>2</sub>, OSC<sub>2</sub>HBr and S<sub>2</sub>C<sub>2</sub>Br<sub>2</sub>).

The choice of molecules limits our test to valence-only correlation as there are no core-valence polarized basis sets (cc-pCVXZ<sup>169</sup> or cc-pwCVXZ<sup>170</sup>) available for Br, which would recover core-valence correlation effects reliably. We have still considered two different valence-correlation schemes, one (A) correlating only valence *s* and *p* electrons (default in Molpro), the other (B) additionally considering 3*d*-electrons of Br (default in Gaussian09<sup>128</sup>). Results obtained with standard correlation-consistent basis sets<sup>163,164,171</sup> are collected in Table 1 for the energy difference  $E(80^\circ) - E(180^\circ)$ .

Regular cc-pVXZ basis sets obviously show erratic results for X=D, but fairly smooth convergence from X=T onwards, towards extrapolated<sup>172</sup> values listed in the table for both correlation schemes (A) and (B). Diffuse-augmentation generally leads to improved results for small basis but to very similar complete basis set (CBS) estimates. Explicitly correlated calculations at the CCSD(T)-F12 level with a triple-zeta basis set finally confirm large basis set and CBS values.

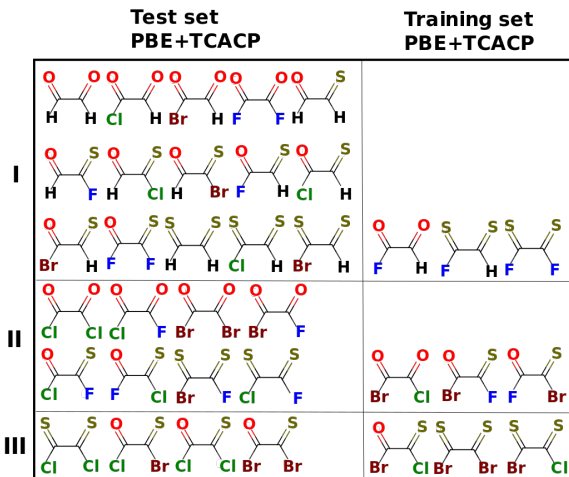


Figure 2: Overview of all molecules. Top, middle and bottom panels correspond to torsional profile classes displayed in Figure 3. Three representative molecules from each class were used to parametrize torsion corrected atom-centered potentials (TCACP) shown in right column.

The fairly smooth convergence of aug-cc-pVXZ<sup>171</sup> for correlation scheme (A) has prompted us to employ valence-*sp*-correlated CCSD(T) with the relatively small aug-cc-pVTZ basis set (also referred to as AVTZ below) as a reference standard for all molecules included in this study (See Fig. 2).

## 3.2 DFT results

### 3.2.1 Overall performance

The reliability of HF and popular DFT functionals was benchmarked against CCSD(T) results for the description of torsional potentials of 36 glyoxal, thiocarbonyl and (methanethioyl)-formaldehyde halides (Fig. 2). Torsional potentials at the CCSD(T) level may be grouped into three classes (Figs. 2 and 3). Systems with light halogens or hydrogen exhibit the conventional minima for *cis* and *trans* conformations that are stabilized by  $\pi$ -conjugation (class I). Substitution with heavier halogens with larger atomic radii introduces steric repulsion,<sup>83</sup> which can only be relieved in non-planar conformations. We observe cases with only one minimum for orthogonal conformations (class III) and intermediate cases where only the *cis*

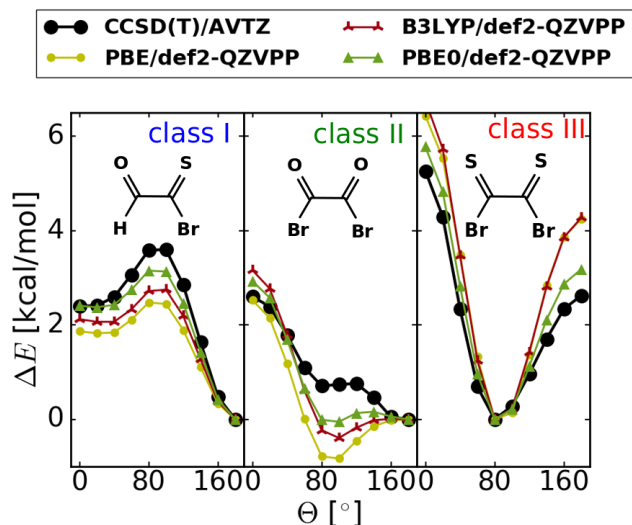


Figure 3: Classification of torsional potentials based on their shape as predicted by CCSD(T). Specific CCSD(T) and DFT results are given for one representative molecule per class.

conformation becomes a transition state (class II). Here the *trans* conformation remains the global minimum and it is typically augmented by a very shallow minimum for nearly orthogonal conformations. Class III compounds always contain at least one sulfur atom as well as chlorine and/or bromine. The very common GGA (PBE, BLYP) and hybrid (B3LYP, PBE0) density functionals are in qualitative agreement with CCSD(T) for classes I and III, but fail to reproduce the shape of class II torsional profiles (Fig. 3).

Before scrutinizing differences between DFT and CCSD(T) one should note that any form of statistical analysis will crucially depend on the choice of reference point for the energy. One may shift DFT and CCSD(T) torsional profiles relative to each other such that the root mean squared deviation between DFT and CCSD(T) energies, sampled along the complete reaction coordinate, is minimized. This would allow for a ranking of functionals in terms of their overall accuracy.

Here we have deliberately chosen a different approach, namely to take that geometry of a molecule as a reference that turns out to be the global minimum at the CCSD(T) level.  $\Delta E$  is then defined to be 0 for that geometry, not

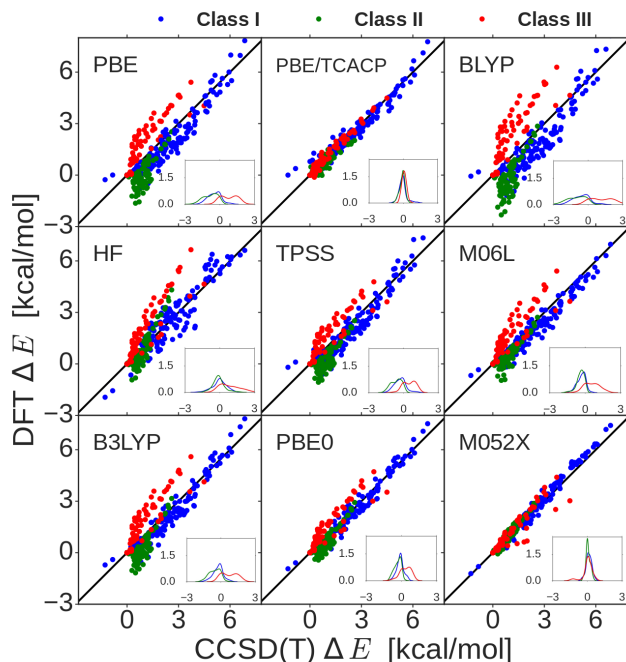


Figure 4: Scatter plots (DFT vs. CCSD(T)) of potential energies of all molecules in Fig. 2 and for ten torsional angles, each relative to the energy for the conformation predicted to be the absolute minimum at the CCSD(T) level. Class I, II, and III profiles are shown in blue, green, and red, respectively. Correspondingly colored error distributions (DFT-CCSD(T)) are shown in insets. See Sec. 3.3 for a discussion of PBE+TCACP.

only at the CCSD(T) level but also at all DFT levels. This choice highlights problems of density functionals to account for the shape of a torsional profile and emphasizes errors in recovering torsional barriers.

Following this choice of reference, Figure 4 shows scatter plots of nine functionals vs. CCSD(T) for all molecules and angles (ten per molecule), as well as corresponding error distributions. Clearly most functionals overestimate the barriers of class III potentials (red) and underestimate them for class I potentials (blue). Their strong bias towards lower energies for class II potentials (green) indicates their tendency to overstabilize orthogonal geometries to the extent that these often become the global minimum (compare with Fig. 3). Particularly serious problems are spotted for GGAs (PBE,

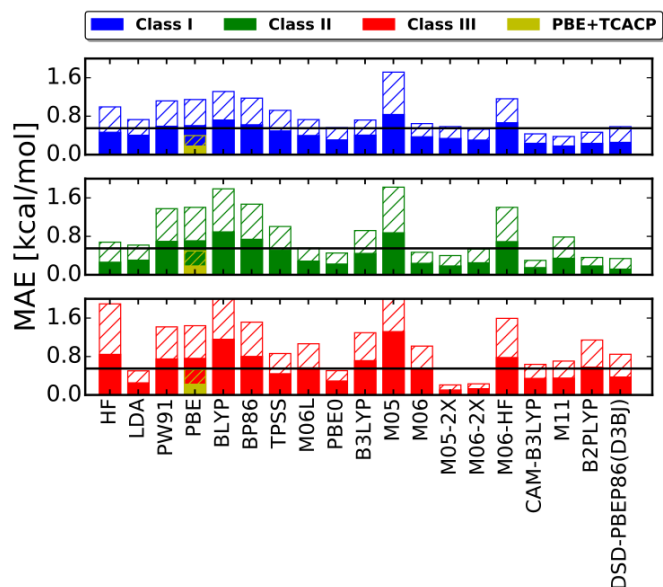


Figure 5: Mean absolute error (MAE, solid bars) and maximum absolute errors per molecule, averaged over all molecules of a given class (MaxAE, shaded bars). See caption of Fig. 4 further details. PBE+TCACP results (Sec. 3.3) are shown in yellow. Solid lines at 0.5 kcal/mol indicate errors that we consider acceptable for reasonable qualitative accuracy.

BLYP), while the highly parametrized M05-2X performs well.

For the same choice of reference point, Figure 5 provides a statistical analysis of HF and DFT energies compared to CCSD(T). Solid color bars illustrate the error averaged over all conformations of all molecules within the corresponding class of torsional profile (MAE, mean absolute error). Shaded color bars indicate the maximum error, found for any conformation of a molecule and averaged over all molecules within a class (MaxAE).

The small energy range of torsional potentials certainly requires an accuracy better than 0.5 kcal/mol in order to ensure a correct description of torsion. LDA shows a surprisingly small MAE of about 0.3 kcal/mol. One would hope for improvement upon climbing "Jacob's ladder"<sup>173</sup>, however, the reverse is true. GGAs clearly perform worse than LDA, and the meta-hybrid M05 shows even larger errors. Large MaxAE values are particularly worrisome for



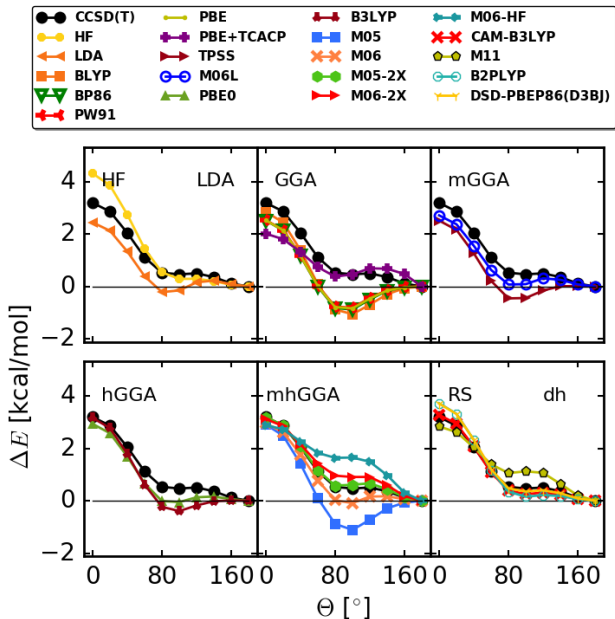


Figure 6: Torsional profile of oxalyl bromide (class II) obtained with popular density functionals and compared to CCSD(T) (in black).

class II profiles, they indicate spurious exaggeration of energy minima at orthogonal confirmation and thus a qualitatively wrong description. The performance of some functionals is still quite satisfactory for particular types of torsional profiles: M05-2X and M06-2X behave well for class III, CAM-B3LYP and the double hybrids (B2PLYP and DSD-PBEP86(D3BJ)) are particularly successful for class I and II. However there seems to be no functional that is universally recommendable for all three types of torsional potential.

Tables 1-3 of Supporting Information 2 list individual energy differences ( $\Delta E$ ) between angles that refer to minima and maxima of the reference CCSD(T) profiles. Mean absolute errors with respect to CCSD(T) are listed as well and largely confirm the main conclusions drawn above: M05-2X and M06-2X reproduce barrier heights of class III molecules very well. CAM-B3LYP falls behind for class III, but is the best performer for classes I and II.

### 3.2.2 Oxalyl bromide

Having assessed the general performance of DFT methods, we now scrutinize results for oxalyl bromide (Fig. 6) as class II representative. CCSD(T) shows a very flat surface between  $\Theta = 80^\circ$  and  $\Theta = 140^\circ$ . Close inspection indicates a very shallow minimum around  $\Theta = 80^\circ$  and an equally shallow transition state at around  $\Theta = 120^\circ$ . Unconstrained optimization at M05-2X/def2QZVPP affords a minimum at  $\Theta = 87.36^\circ$  and a maximum at  $\Theta = 112.93^\circ$ . Subsequent force constant analysis confirms the stationary points to be true a minimum and a true transition state, respectively. The corresponding barrier is very small, however (0.153 kcal/mol), and reduced further at the CCSD(T)/aug-cc-pVTZ//M05-2X/def2QZVPP level (0.04 kcal/mol). A definitive judgment on the existence of these intermediate points is therefore not attainable.<sup>174</sup>

Hartree-Fock behaves reasonably for the overall shape of the potential, but overestimates the *cis* to *trans* barrier; it shows a very flat potential between  $\Theta = 80^\circ$  and  $140^\circ$  without extremal points. Many density functionals, however, predict deep and often global minima for perpendicular geometries. This is observed for LDA as well as for several popular density functionals of various rungs on Jacob’s ladder, including mGGAs (TPSS), hGGAs (PBE0, B3LYP), and mhGGAs (M06, M06-HF). The GGAs (PBE, BLYP, PW91, BP86) and the meta-hybrid M05 functionals perform particularly poorly as they fail to reproduce the *trans*-minimum ( $\Theta = 180^\circ$ ). M06L is the best among the non-hybrid functionals, but only meta-hybrid (M05-2X, M06-2X), range-separated (CAM-B3LYP), and double hybrid (B2PLYP, DSD-PBEP86(D3BJ)) functionals manage to reproduce the finer details of the CCSD(T) reference. Similar remarks about relative performance hold for all molecules of class II and III as well as some cases of class I (all torsional profiles are given in Supporting Information 1).

One possible explanation for the failure of GGA functionals would be the presence of a small HOMO-LUMO gap at  $\Theta \sim 80^\circ$ , responsible for

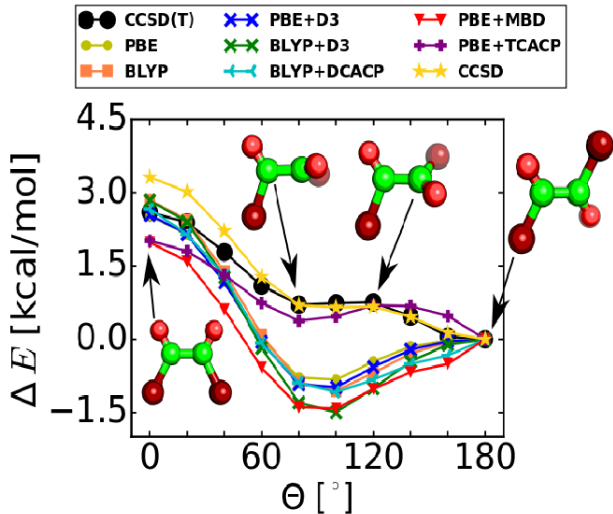


Figure 7: Torsional profile of oxalyl bromide calculated with GGA functionals (PBE, BLYP), with and without TCACP or dispersion corrections (D3, DCACP and MBD), CCSD and CCSD(T).

spurious charge transfer into the lowest unoccupied molecular orbital. However, we calculated a sizable gap of  $\sim 3$  eV ruling out this initial suspicion.

Considering that the interatomic separation between the two Br atoms in oxalyl bromide ranges from 3.3 Å to 4.7 Å in different conformations, one may further suspect a significant contribution of intramolecular dispersion interactions to the shape of torsional profiles. Figure 7 shows torsional profiles calculated using popular dispersion corrections, namely: D3,<sup>148</sup> Many Body Dispersion (MBD)<sup>152</sup> and Dispersion Corrected Atom Centered Potentials (DCACP).<sup>153,154</sup> None of the corrections improve the results of standard GGAs. In fact, they all increase the deviation from CCSD(T). (See also Table 4 in Supporting Information 2). Similar observations have been reported for intramolecular effects in a number of conformers and chemical reactions.<sup>175</sup>

Furthermore, inspection of D3 dispersion corrections reveals maximal contributions for  $80^\circ \leq \theta \leq 100^\circ$ , for which the Br-Br distance approaches the typical van der Waals minimum ( $r_{\text{Br-Br}} \approx 3.7\text{\AA}$ ). This explains the deepening of the spurious minimum. Consequently, lack of dispersion does not cause the observed prob-

lems, it rather lessens them for the wrong reason.

The real culprit instead appears to be the delocalization error. A pragmatic approach to reduce it is to include exact or Hartree-Fock exchange (Hfx). The optimal admixture of exact exchange is  $\sim 50\%$  (also used in the best functionals M05-2X, M06-2X, Figs. 4 - 6). This observation is in agreement with earlier reports for conjugated double bonds.<sup>176,177</sup> Upon increasing the exact exchange further, the accuracy for torsional barriers is impaired again (M06-HF, HF). We tested this further by defining a functional (PBE-2X) that adds 56% of exact exchange to standard PBE. This functional uses the same amount of exact exchange as M05-2X does and Fig. 6 shows that it is almost as accurate as the latter in reproducing the reference CCSD(T) torsional profile of oxalyl bromide. Additional tests indicate that any reduction or increase of exact exchange worsens the results of PBE-2X (data not shown).

### 3.3 TCACP corrections

While some hybrid density functionals (M05-2X, M06-2X, PBE-2X) can provide satisfactory descriptions of torsional profiles, the calculation of exact exchange makes them computationally inefficient for use with plane-wave basis sets. PWs are predominantly employed in condensed phase studies where functionals at the GGA level are a common compromise between efficiency and accuracy. Improvements for GGA based predictions on atom centered corrections (typically implemented in the form of pseudo potentials) were found for various properties, such as London dispersion,<sup>153–155,178,179</sup> vibrational frequencies,<sup>156</sup> band gaps<sup>180–182</sup> and relativistic effects.<sup>183,184</sup> Atom centered corrections have further been used to reduce basis set incompleteness effects.<sup>185</sup> Therefore, we have studied if one can improve the PBE prediction of rotational profiles using custom generated torsion corrected atom centered potentials (TCACP).

Table 2: TCACP parameters [a.u.] for use in PBE functional

	C	O	S	F	Cl	Br
$r_{l=3}$	3.13	1.58	1.82	0.54	0.40	2.41
$h_{11}^{l=3}$	$5.41 \times 10^{-4}$	$-8.06 \times 10^{-3}$	$-6.95 \times 10^{-3}$	$7.04 \times 10^{-4}$	$1.94 \times 10^{-3}$	$-2.18 \times 10^{-3}$

### 3.3.1 Calibration

Torsion corrected effective potentials are optimized for C, O, S, F, Cl and Br (Table 2). As a training set we used 10 energies each along the torsional profiles of nine molecules, selected from all three classes (Fig. 2, right column). The optimized parameters (shown in Table 2) indicate distance  $r_l$  and magnitude  $h_{11}^l$  at which the PBE+TCACP calculations reach maximum agreement with the reference. Note that TCACPs centered on Cl and F peak at  $\sim 0.5$  Bohr from the nuclei, whereas for larger atoms, such as Br, S and O, as well as C,  $r_l$  is larger than 1.5 Bohr (Fig. 8, shown for O, Br, and C in cyan circles). Further note that corrections centered on Br have opposite sign compared to other halogens. A positive (negative)  $h_{11}^l$  indicates that the original PBE exchange-correlation underestimates (overestimates) the reference energy.

### 3.3.2 Electron density

One might expect that TCACPs improve on density functional descriptions through correction of electron densities. Analysis of density differences, however, disproves this hypothesis, at least for the case examined. Although TCACPs successfully eliminate the fairly large energy error for oxalyl bromide at  $\Theta = 80^\circ$  (Fig. 7), as discussed below, the density difference generated (Fig. 8, bottom) is not only much smaller but also largely of opposite sign compared to the one calculated with CCSD as reference (Fig. 8, top). We assume that the use of CCSD instead of CCSD(T) as reference is reasonable, as both methods produce very similar energy curves (Fig. 7). We must, therefore, conclude that TCACPs act directly through a change in the external potential, rather than indirectly through a mediated change of electron

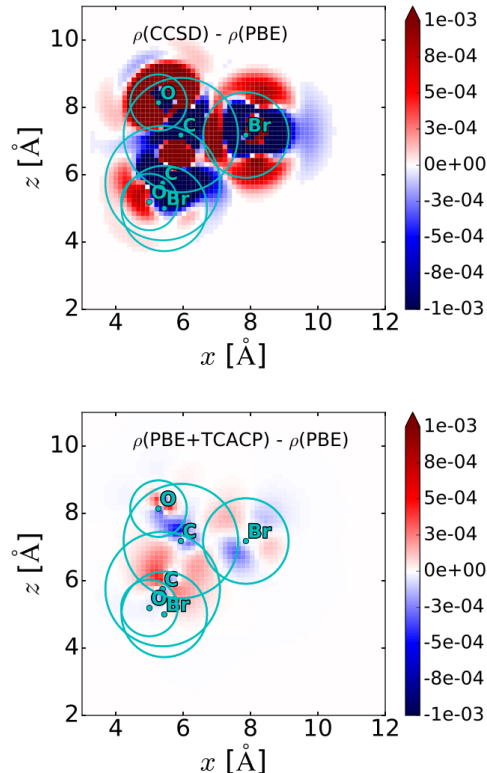


Figure 8: Density difference plots for oxalyl bromide at  $\Theta = 80^\circ$ : PBE versus CCSD (top) and versus PBE+TCACP (bottom). The range at which the TCACPs reach their maximum is illustrated by cyan circles. Isosurface density differences ( $\pm 0.0001$  a.u.) are given as insets.

density.

### 3.3.3 Geometry and frequencies

For general use, it is important to show that TCACPs do not negatively affect other already well-described properties, such as equilibrium geometries and vibrational frequencies. Tests were performed for oxalyl bromide in *cis*, *gauche*, and *trans* conformations (results not shown in detail). Addition of TCACPs changes bond lengths by less than  $0.01$  Å and angles by less than  $0.3^\circ$ . Vibrational frequencies are



affected by  $32\text{ cm}^{-1}$  at most and  $23\text{ cm}^{-1}$  on average. Changes of this order are insignificant for most applications, suggesting that the addition of TCACPs to PBE does not lead to adverse side effects.

### 3.3.4 Torsional profiles

Results obtained from PBE+TCACP are included in Figs. 4, 5 and 7. They all show that TCACPs lead to the desired improvement in the description of rotational profiles. Figure 7 illustrates for oxalyl bromide how TCACPs correct the qualitatively wrong profile and reach good agreement with CCSD(T). The effect is most pronounced for intermediate values of  $\Theta$ . The corrected functional PBE+TCACP still underestimates the barrier by about 1 kcal/mol, but it clearly shows the overall best performance of all GGA functionals. Note that our test case, oxalyl bromide, was not even included in the TCACP training set (Fig. 2). Figure 4, reporting correlations and error distributions, indicates that the corrections are transferable to all molecules included.

Further evidence for the overall good performance of TCACP corrections is obtained from Fig. 5: The relatively large PBE error is reduced to less than 0.5 kcal/mol (black line), which is the threshold we used to identify qualitatively satisfying results. MaxAE is now within the range of 0.5 kcal/mol for all types of torsional profile, which is below the MAE of any of the GGAs, and even lower than some of the hybrid and meta-hybrid functionals. Likewise the MAE for barrier heights (Supporting Information II, Tables 1-3) is among the lowest of all functionals for classes I and II and significantly smaller than PBE also for class III. The complete set of profiles given in the Supporting Information 1 corroborates the overall good performance among all molecules studied here. All these observations suggest that TCACP corrections are a suitable empirical way to rectify some of PBE’s shortcomings in modeling torsional profiles.

### 3.3.5 Intermolecular interactions

After studying the performance of TCACPs for torsional potentials, we were curious to assess their effect on intermolecular interactions. To keep in line with our general choice of test cases, we are again considering oxalyl bromide, now a) in complex with water, b) as a dimer, and c) as a crystal (Fig. 9), which are all thought to benefit from  $\sigma$ -hole-binding.<sup>188</sup> CCSD(T) was used as a binding energy reference in the first two cases but is computationally prohibitive for studying the crystal. No experimental data is available for the cohesive energy of the crystal, restricting us to a qualitative discussion based on the experimental geometry<sup>186,187</sup> only.

PBE underestimates binding energies in all three cases (Fig. 9), and shows hardly any minimum for the oxalyl bromide dimer or the crystal. M05-2X definitely performs better for the complex with water but still falls short of expectations for the dimer. Crystal structure energy evaluation with M05-2X would be computationally too demanding and have thus not been attempted. Dispersion corrections (MBD, D3) remedy the shortcomings of PBE for the water complex and reach the good performance of M05-2X. In the case of PBE, they also lead to an improved description of the dimer. They show little effect for M05-2X. The crystal structure, finally, benefits from dispersion corrections to PBE, as the PBE+MBD energy minimum is now obtained for the experimental lattice constant.

Although parametrized for torsional potentials only, TCACPs also help to improve binding energy curves. They correct the underbinding of the water complex observed with PBE and improve on the description of the dimer and the crystal. Agreement with the CCSD(T) reference for the dimer is actually a little better for PBE+TCACP than for dispersion-corrected PBE, where the crystal lattice constant may be slightly underestimated. Overall both types of correction perform quite similarly. This might indicate that TCACP unintentionally picks up some of the dispersion missing in PBE, at least for the few cases studied here.

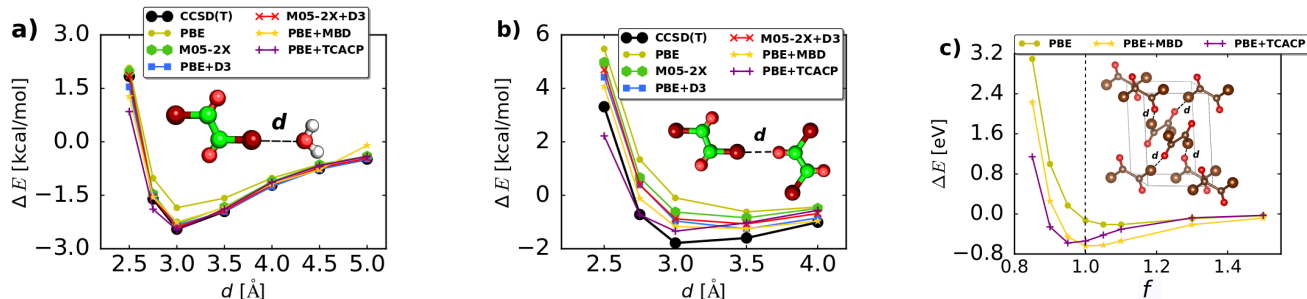


Figure 9: Interaction energy curves of oxalyl bromide with water a), dimer b), and in crystal structure c) obtained using PBE with and without corrections and compared to M052X and CCSD(T) (a, b). Experimental geometry<sup>186,187</sup> has been used in c), and energies are shown as a function of  $f$ , the ratio between assumed and experimental lattice constant.

## 4 Conclusions

An extensive search in literature shows that the performance of density functional approximations for the description of torsional profiles have been mostly tested for systems with small average nuclear charges. Thus, the selection bias on how we test the methods slips cases where the DFT methods fail.

The performance of popular density functional methods was assessed for the description of torsional profiles of 36 molecules: Glyoxal and oxalyl halides, and their thiocarbonyl derivatives. Reference calculations at the CCSD(T) level show that the choice of halogen determines the shape of the profile, and three distinct classes of profile have been identified.

Most density functionals used in this study fail to reproduce barriers accurately and even show qualitatively incorrect profiles for molecules belonging to class II. The initial suspicion that spurious charge transfer might cause the problems could not be substantiated. Lack of dispersion was also ruled out because the tested dispersion corrections (D3,<sup>148</sup> MBD,<sup>152</sup> DCACP<sup>153,154</sup>) only worsened the predictions. Further analysis shows that GGA as well as the meta-hybrid M05 functionals perform worst and that addition of about 50% exact exchange cures most of the problems. Larger amounts of exact exchange tend to impair the accuracy again. The treatment of exchange interactions is thus identified as the core problem of DFT in reproducing torsional barriers of gly-

oxal derivatives substituted with sulfur and/or heavier halogens. This explanation is consistent with the fact that PBE-2X results in a vastly improved rotational profiles for oxalyl bromide. Inclusion of exact exchange, unfortunately, precludes DFT calculations with plane wave basis sets as they demand pure functionals for computational efficiency, particularly in large-scale materials applications. Torsion-corrected atom-centered potentials, TCACPs, have been found to provide a simple, empirical way out of this dilemma. With only 2 parameters per element, they improve the accuracy of standard PBE to a level comparable to the best hybrid functional (M05-2X). TCACPs work well also for molecules outside the training set, and they have little effect on other properties, such as optimized geometries, vibrational frequencies, and electron density distributions. Although parametrized for torsional potentials, TCACPs also improve intermolecular binding potentials, at least for the limited number of test cases studied so far. Thus the design of atom-centered potential corrections which target multiple flaws of GGAs may be a valuable goal in future studies.

## 5 Acknowledgment

The authors thank S. Willitsch, D. Alfè, M. Schwilk, and A. Tkatchenko for suggesting cis-trans isomerism, Quantum Monte Carlo calculations, CCSD(T)-F12 calculations, and discussions, respectively. O.A.v.L. ac-

knowledges funding from the Swiss National Science foundation (No. PP00P2\_138932, 310030\_160067). This research was partly supported by the NCCR MARVEL, funded by the Swiss National Science Foundation. Some calculations were performed at sciCORE (<http://scicore.unibas.ch/>) scientific computing core facility at University of Basel.

## 6 SI

Supporting Information document 1 provides figures with torsional profiles for all molecules and all levels of theory considered in this work. Supporting Information document 2 contains additional tables with (i) individual energy differences ( $\Delta E$ ) between angles that refer to minima and maxima of the reference CCSD(T) profiles as well as MAEs with respect to CCSD(T); (ii) data used to generate Figure 7.

Supporting information document 3 provides all optimized geometries and energies in computer readable format `geometries.txt`.

The Supporting Information is available free of charge on the ACS Publications website.

## References

- (1) Srujana, P.; Gera, T.; Radhakrishnan, T. Fluorescence enhancement in crystals tuned by a molecular torsion angle: A model to analyze structural impact. *J. Mater. Chem. C* **2016**, *4*, 6510–6515.
- (2) Salaneck, W.; Inganäs, O.; Nilsson, J.-O.; Österholm, J.-E.; Themans, B.; Brédas, J.-L. Thermochromism in the poly (3-alkylthiophene)s: A study of conformational defects by photoelectron spectroscopy. *Synth. Met.* **1989**, *28*, 451–460.
- (3) Sorokina, I.; Mushegian, A. The role of the backbone torsion in protein folding. *Biol. Direct* **2016**, *11*, 64–69.
- (4) Fabiano, E.; Della Sala, F. Torsional potential of  $\pi$ -conjugated molecules using the localized Hartree-Fock Kohn-Sham exchange potential. *Chem. Phys. Lett.* **2006**, *418*, 496–501.
- (5) Chen, Y. K.; Wang, Y. A. First-principles computational studies of the torsional potential energy surface of the sec-butyl radical. *Can. J. Chem.* **2011**, *89*, 1469–1476.
- (6) Mo, Y.; Gao, J. Theoretical analysis of the rotational barrier of ethane. *Acc. Chem. Res.* **2007**, *40*, 113–119.
- (7) Bulat, F.; Toro-Labbé, A. A theoretical study of the rotational isomerization of glyoxal and halogen derivatives. *Chem. Phys. Lett.* **2002**, *354*, 508–517.
- (8) Karpfen, A. Torsional potentials of perfluoro-1,3-butadiene and perfluoro-1,3,5-hexatriene: A comparison of *ab initio* and density functional results. *J. Phys. Chem. A* **1999**, *103*, 2821–2827.
- (9) Viruela, P. M.; Viruela, R.; Ortí, E.; Brédas, J.-L. Geometric structure and torsional potential of biisothianaphthene. A comparative DFT and *ab initio* study. *J. Am. Chem. Soc.* **1997**, *119*, 1360–1369.
- (10) Rivero, U.; Meuwly, M.; Willitsch, S. A computational study of the Diels-Alder reactions between 2,3-dibromo-1,3-butadiene and maleic anhydride. *Chem. Phys. Lett.* **2017**, *683*, 598–605.
- (11) Sancho-García, J. C.; Pérez-Jiménez, Á. J.; Moscardó, F. Description of C(sp<sup>2</sup>)-C(sp<sup>2</sup>) rotation in butadiene by density functionals. *J. Phys. Chem. A* **2001**, *105*, 11541–11548.
- (12) Imamura, A.; Hoffmann, R. The electronic structure and torsional potentials in ground and excited states of biphenyl, fulvalene, and related compounds. *J. Am. Chem. Soc.* **1968**, *90*, 5379–5385.
- (13) Bixon, M.; Lifson, S. Potential functions and conformations in cycloalkanes. *Tetrahedron* **1967**, *23*, 769–784.

- (14) Gorenstein, D. G.; Luxon, B. A.; Findlay, J. B. The torsional potential for phosphate diesters: The effect of geometry optimization in CNDO and *ab initio* molecular orbital calculations. *Biochim. Biophys. Acta* **1977**, *475*, 184–190.
- (15) Kveseth, K. A conformational study of some 1,2-disubstituted ethanes by an *ab initio* method. *Acta Chem. Scand. A* **1978**, *32*, 51–56.
- (16) Allinger, N. L.; Profeta, S. The torsional potential function for *n*-butane. *J. Comput. Chem.* **1980**, *1*, 181–184.
- (17) Van-Catledge, F. A.; Allinger, N. L. Torsional potential function of *n*-butane. Correlation effects in the quantum-mechanical prediction of the syn-anti energy difference. *J. Am. Chem. Soc.* **1982**, *104*, 6272–6273.
- (18) Laskowski, B. C.; Jaffe, R. L.; Komornicki, A. Conformational properties, torsional potential, and vibrational force field for methacryloyl fluoride: An *ab initio* investigation. *J. Chem. Phys.* **1985**, *82*, 5089–5098.
- (19) Steele, D. An *ab initio* investigation of the torsional potential function of *n*-butane. *J. Chem. Soc. Faraday Trans. 2* **1985**, *81*, 1077–1083.
- (20) Darsey, J. A.; Thompson, D. L. *Ab initio* molecular orbital calculation of the HONO torsional potential. *J. Phys. Chem.* **1987**, *91*, 3168–3171.
- (21) Carpenter, J. E.; Weinhold, F. Analysis of the geometry of the hydroxymethyl radical by the "different hybrids for different spins" natural bond orbital procedure. *J. Mol. Struct.: THEOCHEM* **1988**, *169*, 41–62.
- (22) Caminati, W.; Damiani, D.; Corbelli, G.; Velino, B.; Bock, C. W. Microwave spectrum and *ab initio* calculations of ethylbenzene: Potential energy surface of the ethyl group torsion. *Mol. Phys.* **1991**, *74*, 885–895.
- (23) Bock, C. W.; Toro-Labbé, A. Theoretical analysis of torsional potential functions: Part II. The rotational isomerization of glyoxal and related molecules. *J. Mol. Struct.: THEOCHEM* **1991**, *232*, 239–247.
- (24) Dixon, D. A. Torsional potential about the central C-C bond in perfluoro-*n*-butane. *J. Phys. Chem.* **1992**, *96*, 3698–3701.
- (25) Guo, H.; Karplus, M. *Ab initio* studies of hydrogen bonding of *N*-methylacetamide: Structure, cooperativity, and internal rotational barriers. *J. Phys. Chem.* **1992**, *96*, 7273–7287.
- (26) Pelz, G.; Yamada, K.; Winnewisser, G. Torsional dependence of the effective rotational constants of H<sub>2</sub>O<sub>2</sub> and H<sub>2</sub>S<sub>2</sub>. *J. Mol. Spectrosc.* **1993**, *159*, 507–520.
- (27) Koput, J.; Seibert, J. W. G.; Winnewisser, B. P. The torsional potential energy function of N<sub>2</sub>O<sub>4</sub>. *Chem. Phys. Lett.* **1993**, *204*, 183–189.
- (28) Hassett, D. M.; Hedberg, K.; Marsden, C. J. The torsional potential for oxalyl chloride: Are there two distinct conformers? *J. Phys. Chem.* **1993**, *97*, 4670–4676.
- (29) Stanton, C. L.; Schwartz, M. *Ab initio* investigation of conformational geometries and the torsional potential surface in perfluorodimethoxymethane. *J. Phys. Chem.* **1993**, *97*, 11221–11226.
- (30) Mannfors, B.; Pietilä, L.-O.; Palmö, K. Torsional potential for the "weak" C(sp<sup>2</sup>)-C(sp<sup>2</sup>) bond in butadiene, biphenyl and styrene. *J. Mol. Struct.* **1994**, *328*, 287–295.
- (31) Röhrlisberger, U.; Klein, M. L. The performance of density functional methods for the description of weak interaction

- potentials. The torsional potential of butane. *Chem. Phys. Lett.* **1994**, *227*, 390–395.
- (32) Hernandez, V.; Lopez Navarrete, J. T. *Ab initio* study of torsional potentials in 2,2'-bithiophene and 3,4'-and 3,3'-dimethyl-2,2'-bithiophene as models of the backbone flexibility in polythiophene and poly(3-methylthiophene). *J. Chem. Phys.* **1994**, *101*, 1369–1377.
- (33) Ortí, E.; Viruela, P. M.; Sánchez-Marín, J.; Tomás, F. *Ab initio* determination of the geometric structure and internal rotation potential of 2,2'-bithiophene. *J. Phys. Chem.* **1995**, *99*, 4955–4963.
- (34) Koput, J. An *ab initio* study on the equilibrium structure and torsional potential energy function of hydrogen peroxide. *Chem. Phys. Lett.* **1995**, *236*, 516–520.
- (35) Klopper, W.; Schütz, M.; Lüthi, H. P.; Leutwyler, S. An *ab initio* derived torsional potential energy surface for (H<sub>2</sub>O)<sub>3</sub>. II. Benchmark studies and interaction energies. *J. Chem. Phys.* **1995**, *103*, 1085–1098.
- (36) Danielson, D. D.; Hedberg, L.; Hedberg, K.; Hagen, K.; Trtiteberg, M. Conformational analysis. 21. The torsional problem in oxalyl chloride. An *ab initio* and electron diffraction investigation of the structures of the conformers and their energy and entropy differences. *J. Phys. Chem.* **1995**, *99*, 9374–9379.
- (37) Koput, J. An *ab initio* study on the equilibrium structure and torsional potential energy function of disulfane. *Chem. Phys. Lett.* **1996**, *259*, 146–150.
- (38) Röthlisberger, U.; Laasonen, K.; Klein, M. L.; Sprik, M. The torsional potential of perfluoro *n*-alkanes: A density functional study. *J. Chem. Phys.* **1996**, *104*, 3692–3700.
- (39) Karpfen, A.; Choi, C. H.; Kertesz, M. Single-bond torsional potentials in conjugated systems: A comparison of *ab initio* and density functional results. *J. Phys. Chem. A* **1997**, *101*, 7426–7433.
- (40) Ivanov, P. M. The torsional energy profile of 1,2-diphenylethane: An *ab initio* study. *J. Mol. Struct.* **1997**, *415*, 179–186.
- (41) Senent, M. *Ab Initio* determination of the roto-torsional energy levels of trans-1,3-butadiene. *J. Mol. Spectrosc.* **1998**, *191*, 265–275.
- (42) Viruela, P. M.; Viruela, R.; Ortí, E. Difficulties of density functional theory in predicting the torsional potential of 2,2'-bithiophene. *Int. J. Quantum Chem.* **1998**, *70*, 303–312.
- (43) Millefiori, S.; Alparone, A. Theoretical study of the structure and torsional potential of pyrrole oligomers. *J. Chem. Soc. Faraday Trans.* **1998**, *94*, 25–32.
- (44) Graf, S.; Leutwyler, S. An *ab initio* derived torsional potential energy surface for the cyclic water tetramer. *J. Chem. Phys.* **1998**, *109*, 5393–5403.
- (45) Cui, S. T.; Siepmann, J. I.; Cochran, H. D.; Cummings, P. T. Intermolecular potentials and vapor-liquid phase equilibria of perfluorinated alkanes. *Fluid Phase Equilib.* **1998**, *146*, 51–61.
- (46) Tsuzuki, S.; Uchimaru, T.; Matsumura, K.; Mikami, M.; Tanabe, K. Torsional potential of biphenyl: *Ab initio* calculations with the Dunning correlation consisted basis sets. *J. Chem. Phys.* **1999**, *110*, 2858–2861.
- (47) Bongini, A.; Bottoni, A. A theoretical investigation of the torsional potential in 3,3'-dimethyl-2,2'-bithiophene and 3,4'-dimethyl-2,2'-bithiophene: A comparison between HF, MP2, and DFT theory. *J. Phys. Chem. A* **1999**, *103*, 6800–6804.



- (48) Rablen, P. R.; Hoffmann, R. W.; Hrovat, D. A.; Borden, W. T. Is hyperconjugation responsible for the "gauche effect" in 1-fluoropropane and other 2-substituted-1-fluoroethanes? *J. Chem. Soc. Perkin Trans. 2* **1999**, 1719–1726.
- (49) Tsuzuki, S.; Houjou, H.; Nagawa, Y.; Hiratani, K. High-level *ab initio* calculations of torsional potential of phenol, anisole, and *o*-hydroxyanisole: Effects of intramolecular hydrogen bond. *J. Phys. Chem. A* **2000**, *104*, 1332–1336.
- (50) Koput, J. The equilibrium structure and torsional potential energy function of methanol and silanol. *J. Phys. Chem. A* **2000**, *104*, 10017–10022.
- (51) Bell, S.; Groner, P.; Guirgis, G. A.; Durig, J. R. Far-infrared spectrum, *ab initio*, and DFT calculations and two-dimensional torsional potential function of dimethylallene (3-methyl-1, 2-butadiene). *J. Phys. Chem. A* **2000**, *104*, 514–520.
- (52) De Oliveira, M. A.; Dos Santos, H. F.; De Almeida, W. B. Structure and torsional potential of *p*-phenylthiophene: A theoretical comparative study. *Phys. Chem. Chem. Phys.* **2000**, *2*, 3373–3380.
- (53) Sancho-García, J. C.; Pérez-Jiménez, Á. J.; Pérez-Jordá, J. M.; Moscardó, F. Torsional potential of 1,3-butadiene: *Ab initio* calculations. *Mol. Phys.* **2001**, *99*, 47–51.
- (54) Arulmozhiraja, S.; Fujii, T. Torsional barrier, ionization potential, and electron affinity of biphenyl - A theoretical study. *J. Chem. Phys.* **2001**, *115*, 10589–10594.
- (55) Federsel, D.; Herrmann, A.; Christen, D.; Sander, S.; Willner, H.; Oberhammer, H. Structure and conformation of  $\alpha,\alpha,\alpha$ -trifluoroanisole,  $C_6H_5OCF_3$ . *J. Mol. Struct.* **2001**, *567–568*, 127–136.
- (56) Shishkov, I. F.; Geise, H. J.; Van Alsenoy, C.; Khristenko, L. V.; Vilkov, L. V.; Senyavian, V. M.; Van der Veken, B.; Herrebout, W.; Lokshin, B. V.; Garkusha, O. G. Trifluoromethoxy benzene in the gas phase studied by electron diffraction and spectroscopy supplemented with *ab initio* calculations. *J. Mol. Struct.* **2001**, *567–568*, 339–360.
- (57) Tsuji, T.; Takashima, H.; Takeuchi, H.; Egawa, T.; Konaka, S. Molecular structure and torsional potential of *trans*-azobenzene. A gas electron diffraction study. *J. Phys. Chem. A* **2001**, *105*, 9347–9353.
- (58) Sancho-García, J. C.; Pérez-Jiménez, Á. J.; Pérez-Jordá, J. M.; Moscardó, F. High-level *ab initio* calculations of the torsional potential of glyoxal. *Chem. Phys. Lett.* **2001**, *342*, 452–460.
- (59) Senent, M. L.; Perez-Ortega, A.; Arroyo, A.; Domínguez-Gómez, R. Theoretical investigation of the torsional spectra of 2,2,2-trifluoroethanol. *Chem. Phys.* **2001**, *266*, 19–32.
- (60) Sakata, K.; Kometani, N.; Hara, K. *Ab initio* calculation of the torsional potential for 2-alkenylanthracene in the ground and excited states. *Chem. Phys. Lett.* **2001**, *344*, 185–192.
- (61) Sancho-García, J. C.; Pérez-Jiménez, Á. J.; Pérez-Jordá, J. M.; Moscardó, F. Characterizing conformers and torsional potentials of nitrosoformaldehyde and *N*-nitrosomethanimine. *J. Chem. Phys.* **2001**, *115*, 3698–3705.
- (62) Sancho-García, J. C.; Pérez-Jiménez, Á. J. A theoretical study of the molecular structure and torsional potential of styrene. *J. Phys. B* **2002**, *35*, 1509–1523.
- (63) Kapustin, E. G.; Bzhezovsky, V. M.; Yagupolskii, L. M. Torsion potentials and

- electronic structure of trifluoromethoxy- and trifluoromethylthiobenzene: An *ab initio* study. *J. Fluorine Chem.* **2002**, *113*, 227–237.
- (64) Tonmuphean, S.; Parasuk, V.; Karpfen, A. The torsional potential of dimethyl peroxide: Still a difficult case for theory. *J. Phys. Chem. A* **2002**, *106*, 438–446.
- (65) Orlandi, G.; Gagliardi, L.; Melandri, S.; Caminati, W. Torsional potential energy surfaces and vibrational levels in *trans* Stilbene. *J. Mol. Struct.* **2002**, *612*, 383–391.
- (66) Pan, J.-F.; Hou, X.-Y.; Chua, S.-J.; Huang, W. Theoretical study of the structure and torsional potential of substituted biphenylenes and their fluorene derivatives. *Phys. Chem. Chem. Phys.* **2002**, *4*, 3959–3964.
- (67) Raos, G.; Famulari, A.; Marcon, V. Computational reinvestigation of the bithiophene torsion potential. *Chem. Phys. Lett.* **2003**, *379*, 364–372.
- (68) Duarte, H. A.; Duani, H.; De Almeida, W. B. *Ab initio* correlated comparative study of the torsional potentials for 2,2'-bipyrrrole and 2,2'-bifuran five membered heterocyclic dimers. *Chem. Phys. Lett.* **2003**, *369*, 114–124.
- (69) Klocker, J.; Karpfen, A.; Wolschann, P. On the structure and torsional potential of trifluoromethoxybenzene: An *ab initio* and density functional study. *Chem. Phys. Lett.* **2003**, *367*, 566–575.
- (70) Klocker, J.; Karpfen, A.; Wolschann, P. Surprisingly regular structure-property relationships between C-O bond distances and methoxy group torsional potentials: An *ab initio* and density functional study. *J. Mol. Struct.: THEOCHEM* **2003**, *635*, 141–150.
- (71) Klocker, J.; Karpfen, A.; Wolschann, P. Trends in the torsional potentials of methoxy and trifluoromethoxy groups: An *ab initio* and density functional study on the structure of para-substituted pyridines and pyridinium cations. *J. Phys. Chem. A* **2003**, *107*, 2362–2368.
- (72) Fliegl, H.; Köhn, A.; Hättig, C.; Ahlrichs, R. *Ab initio* calculation of the vibrational and electronic spectra of *trans*- and *cis*-azobenzene. *J. Am. Chem. Soc.* **2003**, *125*, 9821–9827.
- (73) Cinacchi, G.; Prampolini, G. DFT study of the torsional potential in ethylbenzene and ethoxybenzene: The smallest prototypes of alkyl- and alkoxy-aryl mesogens. *J. Phys. Chem. A* **2003**, *107*, 5228–5232.
- (74) Sakata, K.; Hara, K. *Ab initio* study of the torsional potential for 9-phenylanthracene in the ground and excited states. *Chem. Phys. Lett.* **2003**, *371*, 164–171.
- (75) Halpern, A. M.; Glendenning, E. D. An intrinsic reaction coordinate calculation of the torsional potential in ethane: Comparison of the computationally and experimentally derived torsional transitions and the rotational barrier. *J. Chem. Phys.* **2003**, *119*, 11186–11191.
- (76) Karpfen, A.; Parasuk, V. Accurate torsional potentials in conjugated systems: *Ab initio* and density functional calculations on 1,3-butadiene and monohalogenated butadienes. *Mol. Phys.* **2004**, *102*, 819–826.
- (77) Császár, A. G.; Szalay, V.; Senent, M. L. *Ab initio* torsional potential and transition frequencies of acetaldehyde. *J. Chem. Phys.* **2004**, *120*, 1203–1207.
- (78) Miller III, T. F.; Clary, D. C. Quantum free energies of the conformers of glycine on an *ab initio* potential energy surface. *Phys. Chem. Chem. Phys.* **2004**, *6*, 2563–2571.

- (79) Senent, M. *Ab initio* study of the torsional spectrum of glycolaldehyde. *J. Phys. Chem. A* **2004**, *108*, 6286–6293.
- (80) Sancho-García, J. C.; Karpfen, A. The torsional potential in 2,2'-bipyrrole revisited: High-level *ab initio* and DFT results. *Chem. Phys. Lett.* **2005**, *411*, 321–326.
- (81) Pérez-Jiménez, Á. J.; Sancho-García, J. C.; Pérez-Jordá, J. M. Torsional potential of 4,4'-bipyridine: *Ab initio* analysis of dispersion and vibrational effects. *J. Chem. Phys.* **2005**, *123*, 134309.
- (82) Puzzarini, C.; Taylor, P. R. An *ab initio* study of the structure, torsional potential energy function, and electric properties of disilane, ethane, and their deuterated isotopomers. *J. Chem. Phys.* **2005**, *122*, 054315.
- (83) Kim, S.; Wheeler, S. E.; DeYonker, N. J.; Schaefer, H. F. The extremely flat torsional potential energy surface of oxalyl chloride. *J. Chem. Phys.* **2005**, *122*, 234313.
- (84) Goodman, L.; Sauers, R. R. 1-fluoropropane. Torsional potential surface. *J. Chem. Theory Comput.* **2005**, *1*, 1185–1192.
- (85) Klauda, J. B.; Brooks, B. R.; MacKerell, A. D.; Venable, R. M.; Pastor, R. W. An *ab initio* study on the torsional surface of alkanes and its effect on molecular simulations of alkanes and a DPPC bilayer. *J. Phys. Chem. B* **2005**, *109*, 5300–5311.
- (86) Zhou, Z.-Y.; Jalbout, A. F.; Galano, A.; Solimannejad, M.; Abou-Rachid, H. The FC(O)OF torsional potential: Thermochemistry and kinetics. *J. Mol. Struct.* **2005**, *737*, 83–89.
- (87) Mourik, T. V.; Früchtel, H. A. The potential energy landscape of noradrenaline: An electronic structure study. *Mol. Phys.* **2005**, *103*, 1641–1654.
- (88) Hafezi, M. J.; Sharif, F. Study of the torsional potential energies of 2-methylpropane, *n*-butane, and 2-methylbutane with high-level *ab initio* calculations. *J. Mol. Struct.: THEOCHEM* **2007**, *814*, 43–49.
- (89) Haworth, N.; Gready, J.; George, R.; Wouters, M. Evaluating the stability of disulfide bridges in proteins: A torsional potential energy surface for diethyl disulfide. *Mol. Simul.* **2007**, *33*, 475–485.
- (90) Chowdary, P. D.; Martinez, T. J.; Gruebele, M. The vibrationally adiabatic torsional potential energy surface of *trans*-stilbene. *Chem. Phys. Lett.* **2007**, *440*, 7–11.
- (91) Sturdy, Y. K.; Clary, D. C. Torsional anharmonicity in the conformational analysis of tryptamine. *Phys. Chem. Chem. Phys.* **2007**, *9*, 2065–2074.
- (92) Tsuzuki, S.; Arai, A. A.; Nishikawa, K. Conformational analysis of 1-butyl-3-methylimidazolium by CCSD(T) level *ab initio* calculations: Effects of neighboring anions. *J. Phys. Chem. B* **2008**, *112*, 7739–7747.
- (93) Ovsyannikov, R. I.; Melnikov, V. V.; Thiel, W.; Jensen, P.; Baum, O.; Giesen, T. F.; Yurchenko, S. N. Theoretical rotation-torsion energies of HSOH. *J. Chem. Phys.* **2008**, *129*, 154314.
- (94) de Amorim, M. B. Torsional profile of 2,2,2-trifluoroethanol: A theoretical analysis with basis set extrapolation. *Int. J. Quantum Chem.* **2008**, *108*, 2550–2556.
- (95) Dorofeeva, O. V.; Ferenets, A. V.; Karasev, N. M.; Vilkov, L. V.; Oberhammer, H. Molecular structure, conformation, and potential to internal rotation of 2,6- and 3,5-difluoronitrobenzene studied by gas-phase electron diffraction and

- quantum chemical calculations. *J. Phys. Chem. A* **2008**, *112*, 5002–5009.
- (96) Aquilanti, V.; Ragni, M.; Bitencourt, A. C.; Maciel, G. S.; Prudente, F. V. Intramolecular Dynamics of RS-SR' Systems (R, R' = H, F, Cl, CH<sub>3</sub>, C<sub>2</sub> H<sub>5</sub>): Torsional Potentials, Energy Levels, Partition Functions. *J. Phys. Chem. A* **2009**, *113*, 3804–3813.
- (97) Tuttolomondo, M. E.; Navarro, A.; Peña, T.; Fernández-Liencres, M. P.; Granadino-Roldán, J. M.; Parker, S. F.; Fernández-Gómez, M. New insight into the structure, internal rotation barrier and vibrational analysis of 2-fluorostyrene. *Chem. Phys.* **2009**, *361*, 94–105.
- (98) Newby, J. J.; Müller, C. W.; Liu, C.-P.; Zwier, T. S. Jet-cooled vibronic spectroscopy and asymmetric torsional potentials of phenylcyclopentene. *Phys. Chem. Chem. Phys.* **2009**, *11*, 8330–8341.
- (99) Koroleva, L. A.; Tyulin, V. I.; Matveev, V. K.; Krasnoshchekov, S. V.; Pentin, Y. A. The internal rotation potential functions of the methacryloyl chloride molecule in the ground and excited electronic states. *Russ. J. Phys. Chem. A* **2009**, *83*, 962–966.
- (100) Durig, J. R.; Zhou, S. X.; Zheng, C.; Durig, D. T. Conformational stability, structural parameters and vibrational assignment from variable temperature infrared spectra of xenon and krypton solutions and *ab initio* calculations of ethylisocyanate. *J. Mol. Struct.* **2010**, *971*, 23–32.
- (101) Sıdır, İ.; Sıdır, Y. G.; Kumalar, M.; Taşal, E. *Ab Initio* Hartree-Fock and density functional theory investigations on the conformational stability, molecular structure and vibrational spectra of 7-acetoxy-6-(2, 3-dibromopropyl)-4,8-dimethylcoumarin molecule. *J. Mol. Struct.* **2010**, *964*, 134–151.
- (102) Beames, J. M.; Lester, M. I.; Murray, C.; Varner, M. E.; Stanton, J. F. Analysis of the HOOO torsional potential. *J. Chem. Phys.* **2011**, *134*, 044304.
- (103) Friesen, D. T.; Johnson, R. J. G.; Hedberg, L.; Hedberg, K. Structure and torsional properties of oxalyl chloride fluoride in the gas phase: An electron-diffraction investigation. *J. Phys. Chem. A* **2011**, *115*, 6702–6708.
- (104) Villa, M.; Senent, M. L.; Domínguez-Gómez, R.; Álvarez-Bajo, O.; Carvajal, M. CCSD(T) study of dimethyl-ether infrared and raman spectra. *J. Phys. Chem. A* **2011**, *115*, 13573–13580.
- (105) Castro, M. E.; Muñoz-Caro, C.; Niño, A. Analysis of the nitrile and methyl torsional vibrations of *n*-propyl cyanide in its S<sub>0</sub> electronic state. *Int. J. Quantum Chem.* **2011**, *111*, 3681–3694.
- (106) Blancafort, L.; Gatti, F.; Meyer, H.-D. Quantum dynamics study of fulvene double bond photoisomerization: The role of intramolecular vibrational energy redistribution and excitation energy. *J. Chem. Phys.* **2011**, *135*, 134303.
- (107) Lima, C. F. R. A. C.; Costa, J. C. S.; Santos, L. M. N. B. F. Thermodynamic insights on the structure and energetics of *s*-triphenyltriazine. *J. Phys. Chem. A* **2011**, *115*, 9249–9258.
- (108) Alyar, H.; Bahat, M.; Kantarcı, Z.; Kasap, E. Torsional potential and nonlinear optical properties of phenyldiazines and phenyltetrazines. *Comput. Theor. Chem.* **2011**, *977*, 22–28.
- (109) Hamza, A.; Cable, J. R. Electronic spectroscopy of the *cis* and *trans* isomers of 1-methyl-2-phenylcyclopropane. *Chem. Phys. Lett.* **2012**, *527*, 16–21.

- (110) Lee, N. K.; Park, S.; Yoon, M.-H.; Kim, Z. H.; Kim, S. K. Effect of ring torsion on intramolecular vibrational redistribution dynamics of 1,1'-binaphthyl and 2,2'-binaphthyl. *Phys. Chem. Chem. Phys.* **2012**, *14*, 840–848.
- (111) Qu, C.; Bowman, J. M. Full-dimensional, *ab initio* potential energy surface for  $\text{CH}_3\text{OH} \rightarrow \text{CH}_3 + \text{OH}$ . *Mol. Phys.* **2013**, *111*, 1964–1971.
- (112) Senent, M. L.; Domínguez-Gómez, R.; Carvajal, M.; Kleiner, I. Highly correlated *ab initio* study of the far infrared spectra of methyl acetate. *J. Chem. Phys.* **2013**, *138*, 044319.
- (113) Dakkouri, M.; Typke, V. A theoretical investigation of the structure of 2-nitropyridine-*N*-oxide and the dependency of the  $\text{NO}_2$  torsional motion on the applied wavefunction and basis set. *Struct. Chem.* **2013**, *24*, 1627–1653.
- (114) Napolion, B.; Watts, J. D.; Huang, M.-J.; McFarland, F. M.; McClendon, E. E.; Walters, W. L.; Williams, Q. L. Accurate theoretical predictions for carbonyl diazide molecules: A coupled-cluster study of the potential energy surface and thermochemical properties. *Chem. Phys. Lett.* **2013**, *559*, 18–25.
- (115) Bloom, J. W.; Wheeler, S. E. Benchmark torsional potentials of building blocks for conjugated materials: Bifuran, bithiophene, and biselenophene. *J. Chem. Theory Comput.* **2014**, *10*, 3647–3655.
- (116) Planells, M.; Pizzotti, M.; Nichol, G. S.; Tessore, F.; Robertson, N. Effect of torsional twist on 2nd order non-linear optical activity of anthracene and pyrene tricyanofuran derivatives. *Phys. Chem. Chem. Phys.* **2014**, *16*, 23404–23411.
- (117) Kręglewski, M.; Gulaczyk, I. Inversion-torsional motion in the ethyl radical. *Chem. Phys. Lett.* **2014**, *592*, 307–313.
- (118) Lin, T.-J.; Lin, S.-T. Theoretical study on the torsional potential of alkyl, donor, and acceptor substituted bithiophene: The hidden role of noncovalent interaction and backbone conjugation. *Phys. Chem. Chem. Phys.* **2015**, *17*, 4127–4136.
- (119) Kannengießer, R.; Lach, M. J.; Stahl, W.; Nguyen, H. V. L. Acetyl methyl torsion in *n*-ethylacetamide: A challenge for microwave spectroscopy and quantum chemistry. *ChemPhysChem* **2015**, *16*, 1906–1911.
- (120) Prashanth, J.; Reddy, B. V.; Rao, G. R. Investigation of torsional potentials, molecular structure, vibrational properties, molecular characteristics and NBO analysis of some bipyridines using experimental and theoretical tools. *J. Mol. Struct.* **2016**, *1117*, 79–104.
- (121) Prashanth, J.; Ramesh, G.; Naik, J. L.; Ojha, J. K.; Reddy, B. V. Molecular geometry, NBO analysis, hyperpolarizability and HOMO-LUMO energies of 2-azido-1-phenylethanone using quantum chemical calculations. *Mater. Today: Proceedings* **2016**, *3*, 3761–3769.
- (122) Zakharenko, O.; Motiyenko, R. A.; Aviles Moreno, J.-R.; Jabri, A.; Kleiner, I.; Huet, T. R. Torsion-rotation-vibration effects in the ground and first excited states of methacrolein, a major atmospheric oxidation product of isoprene. *J. Chem. Phys.* **2016**, *144*, 024303.
- (123) Deb, D. K.; Sarkar, B. Theoretical investigation of gas-phase molecular complex formation between 2-hydroxy thiophenol and a water molecule. *Phys. Chem. Chem. Phys.* **2017**, *19*, 2466–2478.
- (124) Shachar, A.; Mayorkas, N.; Sachs, H.; Bar, I. The conformational landscape of 2-(4-fluoro-phenyl)-ethylamine: Consequences of fluorine substitution at the



- para position. *Phys. Chem. Chem. Phys.* **2017**, *19*, 510–522.
- (125) Lin, J. B.; Jin, Y.; Lopez, S. A.; Drucker-erman, N.; Wheeler, S. E.; Houk, K. N. Torsional Barriers to Rotation and Planarization in Heterocyclic Oligomers of Value in Organic Electronics. *J. Chem. Theory Comput.* **2017**, *13*, 5624–5638.
- (126) Goerigk, L.; Hansen, A.; Bauer, C.; Ehrlich, S.; Najibi, A.; Grimme, S. A look at the density functional theory zoo with the advanced GMTKN55 database for general main group thermochemistry, kinetics and noncovalent interactions. *Phys. Chem. Chem. Phys.* **2017**, *19*, 32184–32215.
- (127) Alparone, A. Structural, torsional, vibrational and response electric properties of 2,2'-bitellurophene rotamers. An *ab initio* and density functional theory investigation. *Struct. Chem.* **2014**, *25*, 959–968.
- (128) Frisch, M. J.; Trucks, G. W.; Schlegel, H. B.; Scuseria, G. E.; Robb, M. A.; Cheeseman, J. R.; Scalmani, G.; Barone, V.; Mennucci, B.; Petersson, G. A.; et.al., Gaussian 09, Revision D.01. **2009**, Gaussian Inc., Wallingford, CT.
- (129) Slater, J. C. A simplification of the Hartree-Fock method. *Phys. Rev.* **1951**, *81*, 385–390.
- (130) Vosko, S. H.; Wilk, L.; Nusair, M. Accurate spin-dependent electron liquid correlation energies for local spin density calculations: A critical analysis. *Can. J. Phys.* **1980**, *58*, 1200–1211.
- (131) Perdew, J. P. *Electronic Structure of Solids' 91*, edited by Ziesche, P. and Eschrig, H.; Akademie-Verlag, Berlin, 1991; p 11.
- (132) Perdew, J. P.; Burke, K.; Ernzerhof, M. Generalized gradient approximation made simple. *Phys. Rev. Lett.* **1996**, *77*, 3865–3868.
- (133) Becke, A. D. Density-functional exchange-energy approximation with correct asymptotic behavior. *Phys. Rev. A* **1988**, *38*, 3098–3100.
- (134) Lee, C.; Yang, W.; Parr, R. G. Development of the Colle-Salvetti correlation-energy formula into a functional of the electron density. *Phys. Rev. B* **1988**, *37*, 785–789.
- (135) Perdew, J. P. Density-functional approximation for the correlation energy of the inhomogeneous electron gas. *Phys. Rev. B* **1986**, *33*, 8822–8824.
- (136) Tao, J.; Perdew, J. P.; Staroverov, V. N.; Scuseria, G. E. Climbing the density functional ladder: Nonempirical meta-generalized gradient approximation designed for molecules and solids. *Phys. Rev. Lett.* **2003**, *91*, 146401.
- (137) Zhao, Y.; Truhlar, D. G. A new local density functional for main-group thermochemistry, transition metal bonding, thermochemical kinetics, and noncovalent interactions. *J. Chem. Phys.* **2006**, *125*, 194101.
- (138) Adamo, C.; Barone, V. Toward reliable density functional methods without adjustable parameters: The PBE0 model. *J. Chem. Phys.* **1999**, *110*, 6158–6170.
- (139) Stephens, P. J.; Devlin, F. J.; Chabalowski, C. F.; Frisch, M. J. *Ab initio* calculation of vibrational absorption and circular dichroism spectra using density functional force fields. *J Phys. Chem.* **1994**, *98*, 11623–11627.
- (140) Zhao, Y.; Schultz, N. E.; Truhlar, D. G. Exchange-correlation functional with broad accuracy for metallic and nonmetallic compounds, kinetics, and noncovalent interactions. *J. Chem. Phys.* **2005**, *123*, 161103.
- (141) Zhao, Y.; Truhlar, D. G. The M06 suite of density functionals for main group thermochemistry, thermochemical

- kinetics, noncovalent interactions, excited states, and transition elements: Two new functionals and systematic testing of four M06-class functionals and 12 other functionals. *Theor. Chem. Acc.* **2008**, *120*, 215–241.
- (142) Zhao, Y.; Schultz, N. E.; Truhlar, D. G. Design of density functionals by combining the method of constraint satisfaction with parametrization for thermochemistry, thermochemical kinetics, and noncovalent interactions. *J. Chem. Theory Comput.* **2006**, *2*, 364–382.
- (143) Yanai, T.; Tew, D. P.; Handy, N. C. A new hybrid exchange-correlation functional using the Coulomb-attenuating method (CAM-B3LYP). *Chem. Phys. Lett.* **2004**, *393*, 51–57.
- (144) Peverati, R.; Truhlar, D. G. Improving the accuracy of hybrid meta-GGA density functionals by range separation. *J. Phys. Chem. Lett.* **2011**, *2*, 2810–2817.
- (145) Grimme, S. Semiempirical hybrid density functional with perturbative second-order correlation. *J. Chem. Phys.* **2006**, *124*, 034108.
- (146) Kozuch, S.; Martin, J. M. L. DSD-PBEP86: In search of the best double-hybrid DFT with spin-component scaled MP2 and dispersion corrections. *Phys. Chem. Chem. Phys.* **2011**, *13*, 20104–20107.
- (147) Weigend, F.; Ahlrichs, R. Balanced basis sets of split valence, triple zeta valence and quadruple zeta valence quality for H to Rn: Design and assessment of accuracy. *Phys. Chem. Chem. Phys.* **2005**, *7*, 3297–3305.
- (148) Grimme, S.; Antony, J.; Ehrlich, S.; Krieg, H. A consistent and accurate ab initio parametrization of density functional dispersion correction (DFT-D) for the 94 elements H-Pu. *J. Chem. Phys.* **2010**, *132*, 154104.
- (149) Kresse, G.; Furthmüller, J. Efficient iterative schemes for ab initio total-energy calculations using a plane-wave basis set. *Phys. Rev. B* **1996**, *54*, 11169.
- (150) Kresse, G.; Joubert, D. From ultrasoft pseudopotentials to the projector augmented-wave method. *Phys. Rev. B* **1999**, *59*, 1758.
- (151) Hutter, J.; Curioni, A. Car-Parrinello molecular dynamics on massively parallel computers. *ChemPhysChem* **2005**, *6*, 1788–1793.
- (152) Tkatchenko, A.; DiStasio Jr, R. A.; Car, R.; Scheffler, M. Accurate and efficient method for many-body van der Waals interactions. *Phys. Rev. Lett.* **2012**, *108*, 236402.
- (153) von Lilienfeld, O. A.; Tavernelli, I.; Röthlisberger, U.; Sebastiani, D. Optimization of effective atom centered potentials for London dispersion forces in density functional theory. *Phys. Rev. Lett.* **2004**, *93*, 153004.
- (154) Lin, I.-C.; Coutinho-Neto, M. D.; Felsenheimer, C.; von Lilienfeld, O. A.; Tavernelli, I.; Röthlisberger, U. Library of dispersion-corrected atom-centered potentials for generalized gradient approximation functionals: Elements H, C, N, O, He, Ne, Ar, and Kr. *Phys. Rev. B* **2007**, *75*, 205131.
- (155) von Lilienfeld, O. A.; Tavernelli, I.; Röthlisberger, U.; Sebastiani, D. Variational optimization of effective atom centered potentials for molecular properties. *J. Chem. Phys.* **2005**, *122*, 014113.
- (156) von Lilienfeld, O. A. Force correcting atom centered potentials for generalized gradient approximated density functional theory: Approaching hybrid functional accuracy for geometries and harmonic frequencies in small chlorofluorocarbons. *Mol. Phys.* **2013**, *111*, 2147–2153.

- (157) Goedecker, S.; Teter, M.; Hutter, J. Separable dual-space Gaussian pseudopotentials. *Phys. Rev. B* **1996**, *54*, 1703.
- (158) Nelder, J. A.; Mead, R. A simplex method for function minimization. *Comput. J.* **1965**, *7*, 308–313.
- (159) Giannozzi, P.; Baroni, S.; Bonini, N.; Calandra, M.; Car, R.; Cavazzoni, C.; Ceresoli, D.; Chiarotti, G. L.; Cococcioni, M.; Dabo, I.; et. al., QUANTUM ESPRESSO: a modular and open-source software project for quantum simulations of materials. *J. Phys. Condens. Matter* **2009**, *21*, 395502.
- (160) Purvis III, G. D.; Bartlett, R. J. A full coupled-cluster singles and doubles model: The inclusion of disconnected triples. *J. Chem. Phys.* **1982**, *76*, 1910–1918.
- (161) Raghavachari, K.; Trucks, G. W.; Pople, J. A.; Head-Gordon, M. A fifth-order perturbation comparison of electron correlation theories. *Chem. Phys. Lett.* **1989**, *157*, 479–483.
- (162) Werner, H.-J.; Knowles, P. J.; Knizia, G.; Manby, F. R.; Schütz, M.; Celani, P.; T., K.; Lindh, R.; Mitrushenkov, A.; Rauhut, G.; et. al., MOLPRO, version 2012.1, a package of *ab initio* programs. 2012.
- (163) Dunning Jr, T. H. Gaussian basis sets for use in correlated molecular calculations. I. The atoms boron through neon and hydrogen. *J. Chem. Phys.* **1989**, *90*, 1007–1023.
- (164) Woon, D. E.; Dunning Jr, T. H. Gaussian basis sets for use in correlated molecular calculations. III. The atoms aluminum through argon. *J. Chem. Phys.* **1993**, *98*, 1358–1371.
- (165) Adler, T. B.; Knizia, G.; Werner, H.-J. A simple and efficient CCSD(T)–F12 approximation. *J. Chem. Phys.* **2007**, *127*, 221106.
- (166) Peterson, K. A.; Adler, T. B.; Werner, H.-J. Systematically convergent basis sets for explicitly correlated wavefunctions: The atoms H, He, B–Ne, and Al–Ar. *J. Chem. Phys.* **2008**, *128*, 084102.
- (167) Peterson, K. A.; Figgen, D.; Goll, E.; Stoll, H.; Dolg, M. Systematically convergent basis sets with relativistic pseudopotentials. II. Small-core pseudopotentials and correlation consistent basis sets for the post-d group 16–18 elements. *J. Chem. Phys.* **2003**, *119*, 11113–11123.
- (168) Werner, H.-J.; Knowles, P. J.; Knizia, G.; Manby, F. R.; Schütz, M.; et. al., MOLPRO, version 2015.1, a package of *ab initio* programs. 2015.
- (169) Woon, D. E.; Dunning Jr, T. H. Gaussian basis sets for use in correlated molecular calculations. V. Core-valence basis sets for boron through neon. *J. Chem. Phys.* **1995**, *103*, 4572–4585.
- (170) Peterson, K. A.; Dunning Jr, T. H. Accurate correlation consistent basis sets for molecular core-valence correlation effects: The second row atoms Al–Ar, and the first row atoms B–Ne revisited. *J. Chem. Phys.* **2002**, *117*, 10548–10560.
- (171) Kendall, R. A.; Dunning Jr, T. H.; Harrison, R. J. Electron affinities of the first-row atoms revisited. Systematic basis sets and wave functions. *J. Chem. Phys.* **1992**, *96*, 6796–6806.
- (172) Complete-basis-set extrapolations were performed as suggested for atomization energies in the ATOMIC approach,<sup>?</sup> using the same formulas also for diffuse-augmented basis-sets.
- (173) Perdew, J. P.; Schmidt, K. Jacob’s ladder of density functional approximations for the exchange-correlation energy. AIP Conf. Proc. 2001; pp 1–20.
- (174) Kim et al.<sup>83</sup> have likewise reported a shallow minimum and transition state for

- oxalyl chloride ( $\Theta = 81.7^\circ$  and  $\Theta = 108.9^\circ$ ) with an activation barrier of only 0.09 kcal/mol at the Mp2 level. At M05-2X/def2QZVPP we obtained  $\Theta = 79.83^\circ$  and  $\Theta = 100.81^\circ$ . Single-point calculations at MP2/aug-cc-pVTZ reproduce Kim’s values very closely but also here CCSD(T) indicates a tiny energy differences of 0.019 kcal/mol.
- (175) Goerigk, L. How do DFT-DCP, DFT-NL, and DFT-D3 compare for the description of London-dispersion effects in conformers and general thermochemistry? *J. Chem. Theory Comput.* **2014**, *10*, 968–980.
- (176) Sancho-García, J. C.; Brédas, J.-L.; Cornil, J. Assessment of the reliability of the Perdew–Burke–Ernzerhof functionals in the determination of torsional potentials in  $\pi$ -conjugated molecules. *Chem. Phys. Lett.* **2003**, *377*, 63–68.
- (177) Sutton, C.; Körzdörfer, T.; Gray, M. T.; Brunsfeld, M.; Parrish, R. M.; Sherrill, C. D.; Sears, J. S.; Brédas, J.-L. Accurate description of torsion potentials in conjugated polymers using density functionals with reduced self-interaction error. *J. Chem. Phys.* **2014**, *140*, 054310.
- (178) DiLabio, G. A. Accurate treatment of van der Waals interactions using standard density functional theory methods with effective core-type potentials: Application to carbon-containing dimers. *Chem. Phys. Lett.* **2008**, *455*, 348–353.
- (179) Prasad, V. K.; Otero-de-la Roza, A.; DiLabio, G. A. Atom-Centered Potentials with Dispersion-Corrected Minimal-Basis-Set Hartree–Fock: An Efficient and Accurate Computational Approach for Large Molecular Systems. *J. Chem. Theory Comput.* **2018**, *14*, 726–738.
- (180) Christensen, N. E. Electronic structure of GaAs under strain. *Phys. Rev. B* **1984**, *30*, 5753.
- (181) Segev, D.; Janotti, A.; Van de Walle, C. G. Self-consistent band-gap corrections in density functional theory using modified pseudopotentials. *Phys. Rev. B* **2007**, *75*, 035201.
- (182) von Lilienfeld, O. A.; Schultz, P. A. Structure and band gaps of Ga-(V) semiconductors: The challenge of Ga pseudopotentials. *Phys. Rev. B* **2008**, *77*, 115202.
- (183) Bachelet, G. B.; Schlüter, M. Relativistic norm-conserving pseudopotentials. *Phys. Rev. B* **1982**, *25*, 2103.
- (184) Dolg, M.; Cao, X. Relativistic pseudopotentials: Their development and scope of applications. *Chem. Rev.* **2012**, *112*, 403–480.
- (185) Otero-de-la Roza, A.; DiLabio, G. A. Transferable Atom-Centered Potentials for the Correction of Basis Set Incompleteness Errors in Density-Functional Theory. *J. Chem. Theory Comput.* **2017**, *13*, 3505–3524.
- (186) Groth, P.; Hassel, O. Crystal Structures of oxalyl bromide and oxalyl chloride. *Acta Chem. Scand.* **1962**, *16*, 2311–2317.
- (187) Damm, E.; Hassel, O.; Romming, C. X-ray analysis of (1:1) addition compounds of 1,4-dioxan with oxalyl chloride resp. oxalyl bromide. *Acta Chem. Scand.* **1965**, *19*, 1159–1165.
- (188) Politzer, P.; Murray, J. S.; Lane, P.  $\sigma$ -Hole bonding and hydrogen bonding: Competitive interactions. *Int. J. Quantum Chem.* **2007**, *107*, 3046–3052.

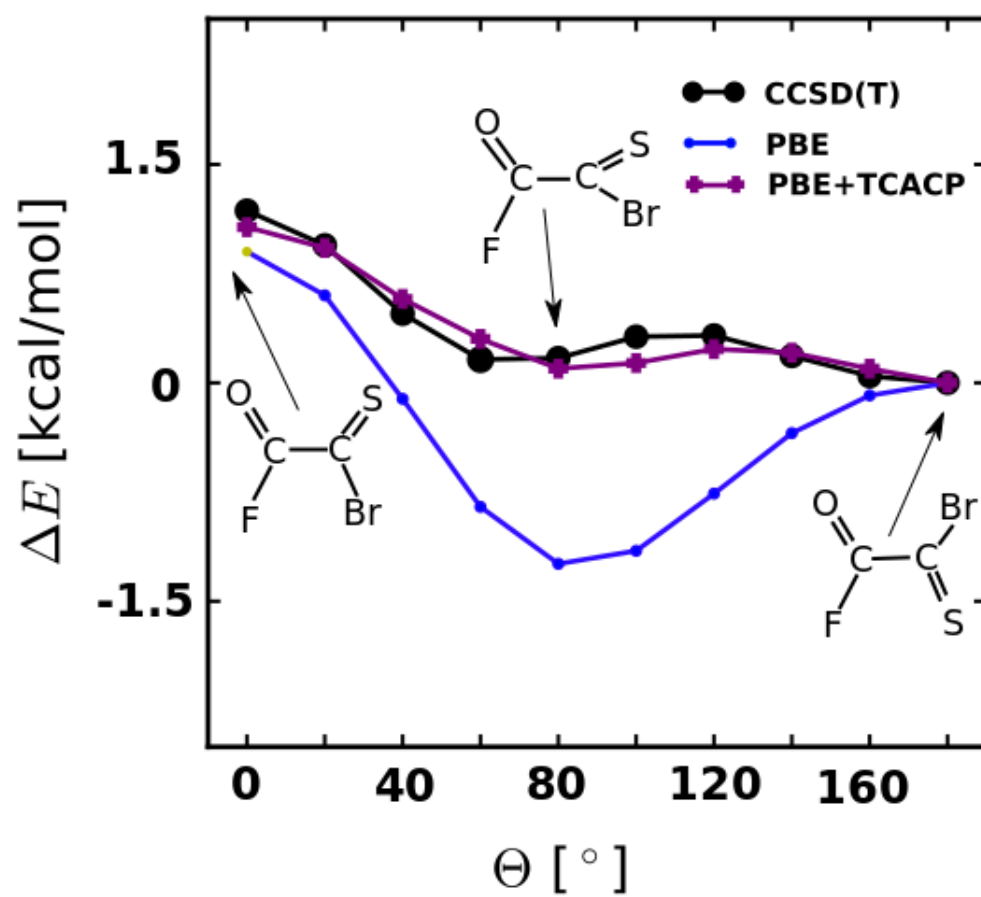


Figure 10: TOC